On the Oxide Ion Conductivity of Potassium Doped Strontium Silicates

Ryan D. Bayliss, [a*†] Stuart N. Cook, [b] Sarah Fearn, [a] John A. Kilner, [a] Colin Greaves [c] and Stephen J. Skinner [a]

[a] Department of Materials, Imperial College London, Prince Consort Road, London SW7 2BP, England

[b] Department of Materials Science and Engineering, Massachusetts Institute of Technology, Cambridge, Massachusetts 02139-4307, U.S.A.

[c] School of Chemistry, University of Birmingham, Birmingham B15 2TT, England

[*] Contact author – Ryan D. Bayliss (rbayliss@uic.edu)

[†] Current address: Department of Chemistry, University of Illinois at Chicago, 845 West Taylor Street, Chicago, 60607, U.S.A.

Recent reports of remarkably high oxygen ion conductivity in a new family of layered strontium silicates have questioned the rationale for materials design in solid electrolytes. Here, we present a re-investigation of the crystal structure, microstructure, total conductivity and perform the first direct investigation of oxygen ion diffusivity of a nominal $Sr_{0.8}K_{0.2}Si_{0.5}Ge_{0.5}O_{2.9}$ composition. The results show very low levels of oxide ion conductivity, which do not correlate with total electrical conductivity. Furthermore, sub-micron elemental mapping reveals a previously unreported inhomogeneous chemical composition. The absence of evidence for secondary phases in the diffraction data suggests that the additional phases are amorphous in nature.

Introduction

Rapid oxide ion conductivity reported by Singh and Goodenough,[1, 2] and subsequently by Martinez *et al*[3] and Wei *et al*[4] in several compositions of monoclinic $Sr_{1-x}A_xMO_{3-}$

$_{0.5x}$ (A = Na, K; M = Si and/or Ge) has recently captured the attention of the energy materials community. These newly proposed superior oxide ion conductors have been reported to possess oxide ion conductivities as high as 1.04 x 10^{-2} S cm^{-1} at 625 °C in the $Sr_{0.8}K_{0.2}Si_{0.5}Ge_{0.5}O_{2.9}$ material. The extraodinarily high values of oxide ion conductivity reported for these phases places them at a level competitive with the state-of-the-art oxide ion conducting ceramics currently used in intermediate temperature solid oxide fuel cells, whilst leaving the possibility of further improvement via chemical and microstructural optimisation.

It is proposed that oxygen vacancy defects are incorporated into these structures via an aliovalent doping strategy (Equation 1) that substitutes Sr with alkali metals (Na or K). This strategy is unusual as alkali metals are typically avoided as dopants in high temperature ceramics due to the high probability of fast ion conduction at low temperatures in solid state materials.

$$K_2O \xrightarrow{SrSiO_3} 2K'_{Sr} + O_O^X + V_O^{\cdot\cdot} \qquad (1)$$

Intriguingly, another Na containing material has recently been discovered to have substantial oxygen ion conductivity, ~1 x 10^{-2} S cm^{-1} at 600 °C, in a family of perovskites based on the ferroelectric $Na_{0.5}Bi_{0.5}TiO_3$ phase,[5] demonstrating that the presence of alkali metals does not preclude pure oxide ion conductivity. However, the authors were rightly cautious of the potential of alkali metal mobility in their novel perovskite phases, directly identifying the dominance of oxide ion conduction by tracer diffusion measurements. Oxygen ions have been assumed as the dominant mobile species in the phases proposed by Singh and Goodenough,[1, 2] even though, no direct determination or evidence of oxygen ion conductivity has been reported.

Of further interest is the apparent absence of dopant defect interactions in these systems. Cation substitution typically introduces defect interactions, related to both charge and ionic radius differences on the cation site. These materials appear to have negligible effects from defect pinning with increasing substitutional content. This is remarkably demonstrated in the Na doped $SrSiO_3$-type phase with a continuous increase in conductivity up to 45 at% Na present on the Sr site, the highest Na concentration reported to date. Acceptor doped oxides typically produce a conductivity maxima at signficantly lower substitutional levels,[6, 7] which is associated with the formation of dimer and trimer associates,[8] but higher order clusters are possibly leading to the formation of nano-domains of secondary phases.

In this work, we report the refined crystal structure of the highest conducting K doped phase, nominally $Sr_{0.8}K_{0.2}Si_{0.5}Ge_{0.5}O_{2.9}$, and investigate the concentration of defects on oxygen sites based on time-of-flight neutron powder diffraction (NPD). Furthermore, we re-investigate the total electrical conductivity (bulk and grain boundary) by electrochemical impedance spectroscopy and directly determine the oxygen ion diffusion coefficient using the Isotope Exchange Depth Profiling (IEDP) technique, in conjunction with Time-of-Flight Secondary Ion Mass Spectrometry (ToF-SIMS).[9, 10] The use of ToF-SIMS also allowed the study of bulk elemental distribution.

Experimental

The samples of $Sr_{0.8}K_{0.2}Si_{0.5}Ge_{0.5}O_{2.9}$ produced during this work were synthesised from $SrCO_3$ (Sigma-Aldrich >99.9%), K_2CO_3 (Sigma-Aldrich 99.995%), SiO_2 (Sigma-Aldrich >99.9%) and GeO_2 (Alfa Aesar 99.98%), as in the literature ,[1] with heating/cooling rates of 300 °C hr^{-1}. Inductively Coupled Plasma – Atomic Emission Spectroscopy (ICP-AES) was performed to confirm the bulk elemental stoichiometry of these samples at the Natural History Museum, London, UK. These values were

compared to elemental standards of known concentration. Pellets were prepared by uniaxial pressing of the powder with ~3 tons of pressure, followed by isostatic pressing at ~300 MPa before sintering.

NPD data were obtained via the GEM Xpress service at ambient temperature on the GEM diffractometer at ISIS, Oxford, UK. Total data collection time was approximately 2 hours. The high resolution bank (backscattered detector) was used for analysis in the structural work presented here. The General Structure Analysis Program GSAS[11] was used for Rietveld structure refinements, in conjunction with the user interface EXPGUI for both X-ray and neutron diffraction data.[12] Diffraction measurements were performed on the as-synthesised powder. The crystalline fraction of a sample prepared in a similar fashion to that described in detail in this paper was estimated by preparing X-ray diffraction samples containing a well-defined percentage of an alumina reference material and calculating the crystalline phase fraction using a 2-phase GSAS refinement.

Two-point AC impedance spectroscopy measurements were performed on pellets in dry flowing air to examine the total conductivity (bulk and grain boundary) as a function of temperature using a Solartron 1260 frequency response analyser. Measurements were made in the frequency range of 1 Hz to 10 MHz with an AC amplitude of 10 mV. Platinum electrodes were painted onto the entire surface of the pellets (typical sample diameter ~12 mm, length ~0.125 mm) and sintered at 900 °C for 1 hour. The sample was held in good contact with the Pt electrode wires by a spring mechanism during the experiment. The total sample conductance at each temperature was determined by the high frequency intercept of the electrode arc with the real Z’ axis. An example AC impedance spectra can be found in the supplementary information (Figure S1).

For IEDP measurements, samples were first polished to a 4 μm finish, limited by the hygroscopic nature of the materials, and oxygen surface exchange was catalysed by a porous Pt coating (~50 nm) on the polished surface. The sample was pre-annealed in an oxygen atmosphere (pO_2 = 200 mbar) with a natural isotopic abundance at the temperature of interest, for at least 10 times the length of the exchange anneal. The sample was then quenched, and the atmosphere replaced with dry ^{18}O-enriched oxygen (pO_2 = 200 mbar, [^{18}O] = 95%) and then annealed for a duration of 72 minutes at 737 °C. Sample density was ~96% of the theoretical value. The surface activated with Pt was sintered at 900 °C for 1 hour *in situ* prior to the pre-anneal. The porosity of the Pt microstructure was confirmed by scanning electron microscopy after the exchange. An IONTOF ToF-SIMS 5 was used to analyse the samples using a 25 keV Bi^+ analytical ion beam with a 2 keV O_2^+ sputter beam for ion mapping, and a 2 keV Cs^+ sputter beam for cleaning during ^{18}O mapping of the sample cross section. A low energy electron flood gun was used for charge compensation. During chemical and isotopic mapping the SIMS instrument was operated under an analysis mode that facilitates a lateral resolution of approximately 200 nm.

Results and Discussion

Due to concerns regarding the retention of K within the structure during high temperature sintering conditions, elemental analysis has been performed against standards on powders prepared from crushed pellets of $Sr_{0.8}K_{0.2}Si_{0.5}Ge_{0.5}O_{2.9}$. Within experimental error, all cation ratios were as expected, relative to the nominal bulk chemical composition.

A Rietveld structural refinement was performed on the powdered sample using energy-dispersive NPD data, allowing reliable quantification of oxygen vacancy concentrations. The initial structural model was based on the monoclinic $SrSiO_3$ cell,[13]

in which the atomic coordinates of each mixed Sr/K and Si/Ge site were constrained as equivalent, while both the Sr/K and both the Si/Ge sites were constrained to have equal atomic displacement parameters. The fractional occupancies of the cation sites were ideally mixed on each site and constrained to the nominal chemical composition, supported by the ICP-AES analysis. Initial lattice cell parameters were obtained from the literature[1] for the composition under investigation and the structural refinement achieved a reasonably good fit within several refinement cycles.

However, on attempting to refine the ratios of cations on the A-site (Sr/K), much improved statistical fits could be achieved from structures with K absent and a lower concentration of oxygen vacancies present. The Rietveld analysis presented here suggests that K is not present in the crystal structure. Interestingly, the absence of Na has also been noted in the nominal phase $Sr_{0.55}Na_{0.45}SiO_3$, and the results of this study will be published elsewhere.[14]

The final structural parameters for the K-free Rietveld fit (Figure 1) can be seen in Table 1. Lattice cell parameters of a = 12.4481(5) Å, b = 7.2126(3) Å, c = 11.0526(4) Å, β = 111.455(2) ° were obtained, remarkably similar to those reported by Martinez *et al* also using powder neutron diffraction for the 20 atomic % K-doped phase.[3] During the refinement, the atomic sites were refined with respect to their fractional coordinates, anisotropic atomic displacement parameters and site occupancy, the latter of which shows a small concentration of vacancies present on both Sr and O sites. Figure 2 presents the crystal structure resulting from the Rietveld refinement, indicating the layers of $(Si/Ge)_3O_9$ tetrahedra are separated by close packed layers of Sr ions parallel to the *ab* plane.

Some sample shape deformation was observed in high-density pellets (>95% of the theoretical density) suggesting that the sintering temperature is close to the melting

point. However, the crystal structure appears to remain unchanged based on powder X-ray diffraction data obtained both before and after sintering. The identification of K from ICP-AES results, combined with its absence in the Rietveld refinements may suggest the presence of a secondary amorphous phase. Potassium silicate is a glass-forming silicate with the general formula K_2SiO_3, of which a small amount would be hard to detect in the background of a highly crystalline phase. The NPD background does not show any strong evidence of diffuse peaks so direct evidence of an amorphous phase cannot readily be deduced from this method. Therefore, the presence of an amorphous component was quantified for a sample synthesised in a similar way with a nominal 20% of Sr substituted by K. Two XRD samples were prepared containing 35% and 50% by weight of standard Al_2O_3; two-phase Rietveld refinement gave the actual weight percentage of the two crystalline components. These data indicated a substantial amount of a non-crystalline component: 47% and 41% for the two samples. The nature of this component remains unclear without further detailed study. It is worth noting that the values for non-crystalline content could be artificially enhanced to a small degree due to the water absorption previously mentioned. In general alkali silicate glasses with composition K_2O:SiO_2 or Na_2O:SiO_2 can be made to crystallise by holding them just below their melting points for long periods of time, however they are more commonly found in the glassy phase, where non-stoichiometric compounds with large variations in the alkali metal to silicate ratio are possible.[15]

As noted by Singh and Goodenough,[2] the nominally $Sr_{1-x}K_xSi_{1-y}Ge_yO_{3-0.5x}$ samples are highly hygroscopic. During this work an increase in mass of 6 % was recorded in just 48 hours in static air. The hygroscopic nature of the material resulted in the dense pellets breaking down into powders when exposed to the laboratory atmosphere for any substantial period of time (> 1 month). This result could be explained by the

presence of potassium silicates, which are known to be highly hygroscopic and to expand significantly with water incorporation.[16, 17] Therefore, to prevent any moisture interfering with the nominally dry experiments, samples were kept in desiccators and were heated to high temperatures, typically 750 - 800 °C, for several hours *in situ* prior to all measurements.

Electrodes were initially prepared by painting Ag paste on to the pellet surfaces followed by sintering at 700 °C for 1 hour. However, the use of Ag produced significantly higher sample resistance, suggesting the possibility of reaction between the Ag paint and the sample. Visual inspection of cross-sections of these samples following thermal treatment revealed dark colour profiles extending from each electrode, suggesting the possibility of Ag diffusion through the material, though no obvious diffusion profile for Ag could be obtained by ToF-SIMS. However, this could be explained by the low ionisation yield of Ag in SIMS, making it difficult to detect. Pt was found to be more stable on the surface of the samples, with no evidence of reaction during the measurements performed at temperatures of up to 900 °C.

For the electrical measurements, the samples were initially heated *in situ* to the highest measurement temperature and held for 6 hours before continuing the experiment. The sample was held at each experimental temperature for a period of 1 hour to ensure thermal equilibration. The sample temperature was measured using an independent K-type thermocouple positioned next to the sample in the furnace. Measurements were performed on cooling only, in order to avoid issues associated with the absorption of water.

Importantly, the electrical resistance data collected during this work has shown the total conductivity (bulk and grain boundary) to be significantly lower than that initially reported by Singh and Goodenough for the same composition.[1] An example fitting of

the impedance spectra to the equivalent circuit can be found in the supplementary information (Figure S1). Analysis of the capacitance values (~10^{-12} F) suggest the response is related to bulk behaviour, not blocking grain boundaries. Should this component represent the entirety of the sample the relative permittivity would be very low at ~ 1.2. Given the inhomogeneous, composite-like nature of the sample, as we reveal later, this would perhaps relate to a smaller fraction of the sample which would significantly raise the calculated permittivity. The near-45° slope seen in the low frequency component may correspond to a diffusion process in the sample caused by blocking electrode behaviour, which would be consistent with the long-time DC behaviour and the low transference number discussed later in this work.

Figure 3 shows an Arrhenius plot of total conductivity versus reciprocal temperature for the previously reported data[1] and those obtained in this work; this shows the conductivity values for the latter are typically greater than one order of magnitude lower. These differences are beyond that typically expected from experimental variation. In order to confirm total conductivity, two point DC measurements were performed on the same sample in another experimental setup. Although an identical resistivity to the ac determination, within error, was found initially, the resistivity increased by ~ 4 orders of magnitude after a few minutes. This strongly suggests that oxygen ion migration is not the predominant transport mechanism in this material.

A clear transition in the temperature dependence at 600 – 700 °C is seen in both the data collected during this work and the literature reported values.[1] Both the high and low temperature regimes have almost identical activation energies in each set of results, however the data in this work shows a much more significant transitional jump.

In order to investigate the oxygen ionic fraction of total conductivity, effectively the oxygen ion transference number of this sample, isotope exchange depth profiling has been performed.

Oxygen tracer diffusion experiments have been a key technique in the development of fuel cell materials, allowing the direct determination of the oxygen ion self-diffusion coefficient, (D^*) as well as determining the oxygen surface exchange kinetics (k).[18-20] Assuming the measured conductivity is entirely ionic in nature, isotope exchange anneal parameters can be established in order to achieve an easily measured diffusion profile length of ~100 μm. These were calculated as an exchange anneal time of 10 min at a temperature of 600 °C. Initial results showed that without the use of a catalysing surface coating, the ^{18}O concentration was too low to be resolved from natural isotopic abundance by ToF-SIMS anywhere in the sample. This does not immediately indicate the lack of oxygen diffusion but merely that the surface exchange kinetics of this material are relatively poor. Utilising a porous Pt coating allowed the identification of ^{18}O enrichment at the surface, however, the depth to which it diffused was not enough to distinguish it from the surface roughness of a few μm. The exchange anneal duration was therefore extended and the temperature raised in order to facilitate the quantification of a diffusion coefficient. The resultant oxygen tracer diffusion profile obtained from $Sr_{0.8}K_{0.2}Si_{0.5}Ge_{0.5}O_{2.9}$ is reported in **Figure 4** for an exchange time of 72 minutes at 737°C. The apparent diffusion profile length is approximately 5 μm, which extends but a few microns beyond the surface roughness, as determined from the Pt^- ion profile obtained simultaneously. While the normalised ^{18}O surface concentration is high at ~30 %, indicating that surface exchange was indeed catalysed, the lack of migration away from the surface reveals that this material exhibits almost no oxide ion diffusivity. Although it cannot be completely isolated

from the effect of surface roughness, the oxygen ion diffusion profile in Figure 4 was fitted to Crank's solution to Fick's second law of diffusion for a semi-infinite medium,[21] resulting in a very low oxygen ion self-diffusion coefficient, D^*, of 6.5 x 10^{-12} cm^2 s^{-1}. For comparison, Gd-doped CeO_2 has a typical D^* of ~2 x 10^{-7} cm^2 s^{-1} at 700 °C,[19] which would result in a diffusion length of approximately 600 µm after the exchange anneal duration of 72 minutes. While the accuracy of this measurement is limited by our ability to make planar surfaces and the requirement for catalysed surface exchange, it does however present an effective upper limit for diffusion in this material at 737 °C.

Considering the low oxygen diffusion coefficient and the relatively high total conductivity data reported in Figure 3, the Nernst-Einstein relationship can be used to obtain a transference number for oxygen ion conductivity, allowing both measurements to be directly compared. Using a calculated charge carrier concentration of 3.8 x 10^{22} oxygen atoms per cm^{-3} based on the formula $Sr_{0.8}K_{0.2}Si_{0.5}Ge_{0.5}O_{2.9}$, effectively the maximum charge carrier concentration possible assuming vacancy migration, we obtain a total oxygen ion conductivity of 1.8 x 10^{-6} S cm^{-1}. This low value of total oxygen ion conductivity results in a transference number of 3 x 10^{-3} (based on a total electrical conductivity of 5 x 10^{-3} S cm^{-1}), leading us to the conclusion that the majority of the conductivity in this material is not due to oxygen ions migrating in the bulk of the material.

Finally, whilst initially focusing on the oxygen negative spectra recorded from the ToF-SIMS experiments, a study of the overall chemical ion distribution revealed a surprising microstructural feature previously unreported for these doped strontium silicates. **Figure 5** shows quite clearly the phase separation observed on studying the positive ion yields of a polished cross sectional area of a typical pellet of nominal

chemical composition $Sr_{0.8}K_{0.2}Si_{0.5}Ge_{0.5}O_{2.9}$. This variation in chemical composition shows two principle regions which would correspond to at least a Sr(Si/Ge) type oxide and a K(Si/Ge) type oxide phase. The latter of which we associate with the previously mentioned K_2SiO_3 type glass that would be hard to observe in the background of the diffraction and data and may explain why it has been previously undetected. The presence of less abundant regions dominated by just Si and O signals is also observed.

It is worth noting, during ToF-SIMS analysis of the oxygen isotope diffusion profiles, variations in oxygen diffusion coefficients (less than an order of magnitude greater diffusion length than the "bulk" measurement) were identified which were generally considered to be characteristic of low density materials and attributed to percolating pores. However, with the new knowledge of the sample's chemical inhomogeneity, we cannot preclude that one of the phases present does not in fact have higher oxygen diffusivity than that determined to be bulk. The diffusivity of this pathway, if it percolates through the sample, is still very low with respect to total conductivity. A map of the isotopic ratio across a $150 \times 150\ \mu m^2$ region can be seen in Figure S2 in the supplementary information. The inhomogeneity of the diffusion front is on the same scale as that of the chemical distribution reported in Figure 5.

Further work to be published subsequently will show that the $Sr_{0.55}Na_{0.45}SiO_3$ composition, the highest performing member of the family reported by Singh and Goodenough,[2] exhibits an identical dopant-free crystal structure yet similarly reduced conductivity, oxygen diffusivity and chemical inhomogeneity.

Conclusions

The phase with nominal composition $Sr_{0.8}K_{0.2}Si_{0.5}Ge_{0.5}O_{2.9}$ with proposed fast oxygen ion conduction has been synthesised and the chemical composition and crystal structure re-investigated by ICP-AES and NPD. A Rietveld refinement of NPD data

suggests no K is present in the crystalline part of the material, but indicates a small concentration of Sr vacancies exist, which results in a low concentration of oxygen vacancies. A microstructural investigation by ToF-SIMS chemical ion mapping has shown that the material comprises of at least two phases, tentatively suggesting a crystalline $SrSi_{1-x}Ge_xO_3$ and an amorphous potassium silicate component.

A re-investigation of total conductivity (bulk and grain boundary) by AC impedance spectroscopy reveals lower values than previously reported, despite the samples exhibiting nominally identical bulk chemistry and crystal structure. Finally, IEDP has been performed showing no evidence of significant oxygen ion diffusion.

The reported high performance of these materials in the fuel cell environment suggests the presence of rapid ionic migration, however whilst this work has been unable to determine the species responsible for the high conductivity, we suggest that it is not related to oxygen ion migration. While these materials, even if they are considered composites, remain of great interest, without full understanding of the correct charge carrier it will be difficult to chemically optimise the materials further. This clearly demonstrates that further work is now needed to determine the correct charge carrier in the materials responsible for high conductivity.

Acknowledgements

The authors would like to thank the referees for their comments which have proved useful in clarifying and refining this work. R. D. B. and S. J. S. would like to thank Prof Peter R. Slater and Dr Tom Baikie for useful discussion and comments on the manuscript. R. D. B would like to thank Prof Jordi Cabana for providing resources to complete the work. The authors would like to thank Dr Emma Williams at the Natural History Museum for her assistance with the ICP-AES. The authors thank Dr Ron Smith

for the rapid NPD data collection (XB 1290087) via the GEM Xpress access route at ISIS, Rutherford Appleton Laboratories, Chilton, Didcot, UK.

References

1. P. Singh and J. B. Goodenough, *Energ Environ Sci*, 2012, **5**, 9626-9631.
2. P. Singh and J. B. Goodenough, *J Am Chem Soc*, 2013, **135**, 10149-10154.
3. R. Martinez, P. Singh, J. A. Alonso and J. B. Goodenough, *Journal of Materials Chemistry A*, 2014.
4. T. Wei, P. Singh, Y. Gong, J. B. Goodenough, Y. Huang and K. Huang, *Energ Environ Sci*, 2014.
5. M. Li, M. J. Pietrowski, R. A. De Souza, H. Zhang, I. M. Reaney, S. N. Cook, J. A. Kilner and D. C. Sinclair, *Nat Mater*, 2014, **13**, 31-35.
6. J. A. Kilner, *Solid State Ionics*, 2000, **129**, 13-23.
7. J. A. Kilner, *Solid State Ionics*, 1983, **8**, 201-207.
8. P. S. Manning, J. D. Sirman, R. A. DeSouza and J. A. Kilner, *Solid State Ionics*, 1997, **100**, 1-10.
9. R. A. De Souza, J. Zehnpfenning, M. Martin and J. Maier, *Solid State Ionics*, 2005, **176**, 1465-1471.
10. R. J. Chater, S. Carter, J. A. Kilner and B. C. H. Steele, *Solid State Ionics*, 1992, **53**, 859-867.
11. A. C. Larson and R. B. Von Dreele, Los Alamos National Laboratory Report LAUR 86-748, 1994.
12. B. H. Toby, *J Appl Crystallogr*, 2001, **34**, 210-213.
13. F. Nishi, *Acta Crystallogr C*, 1997, **53**, 534-536.
14. R. D. Bayliss, S. N. Cook, S. Fearn, C. Greaves, J. A. Kilner and S. J. Skinner, *In preparation*.
15. G. Lagaly, W. Tufar, A. Minihan and A. Lovell, in *Ullmann's Encyclopedia of Industrial Chemistry*, Wiley-VCH Verlag GmbH & Co. KGaA, 2000.
16. K. B. Langille, D. Nguyen, J. O. Bernt, D. E. Veinot and M. K. Murthy, *J Mater Sci*, 1991, **26**, 704-710.
17. K. B. Langille, D. Nguyen, J. O. Bernt, D. E. Veinot and M. K. Murthy, *J Mater Sci*, 1991, **26**, 695-703.
18. A. V. Berenov, A. Atkinson, J. A. Kilner, E. Bucher and W. Sitte, *Solid State Ionics*, 2010, **181**, 819-826.
19. E. Ruiz-Trejo, J. D. Sirman, Y. M. Baikov and J. A. Kilner, *Solid State Ionics*, 1998, **113**, 565-569.
20. S. J. Skinner and J. A. Kilner, *Solid State Ionics*, 2000, **135**, 709-712.
21. J. Crank, *The mathematics of diffusion*, Clarendon Press, Oxford, 1975.

Figures & Tables

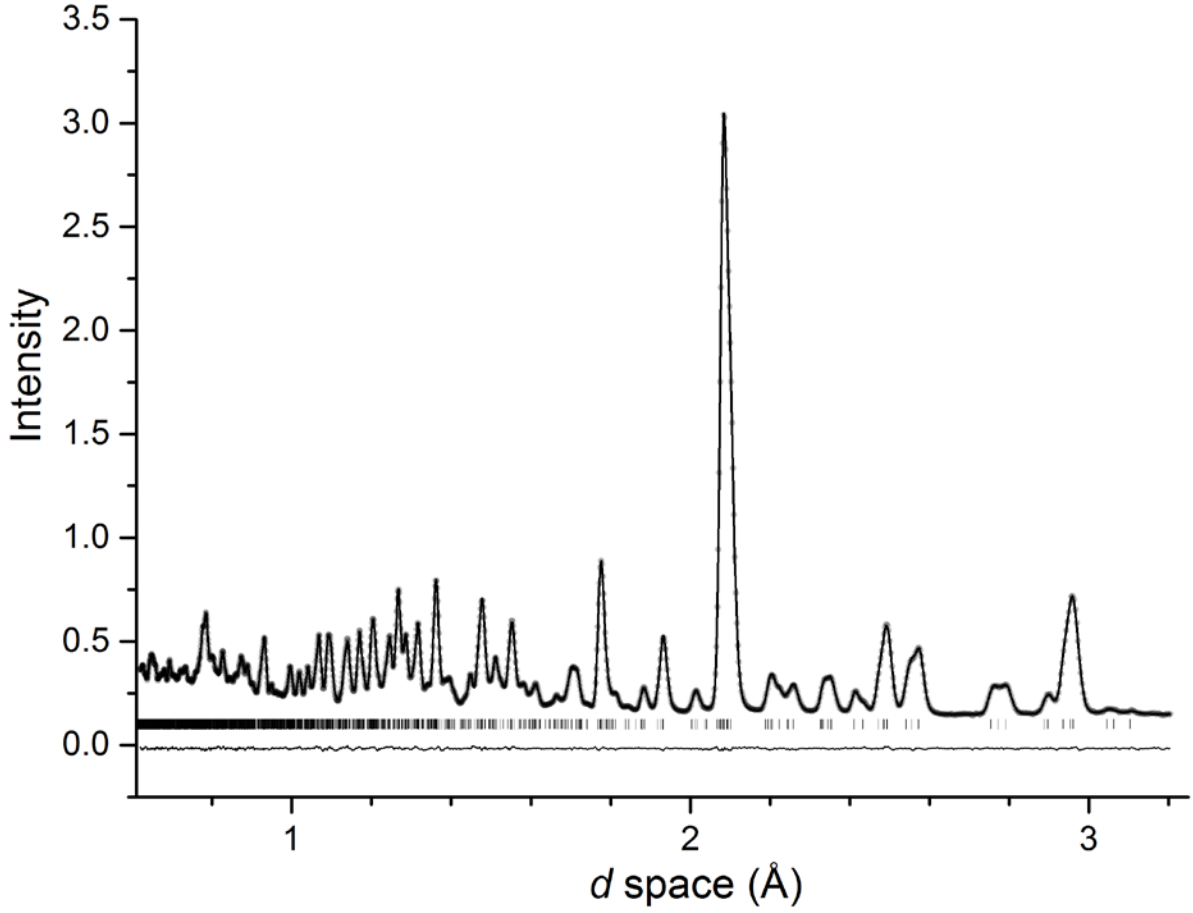

Figure 1. Final Rietveld fit of ambient temperature time-of-flight neutron powder diffraction data showing observed data (●), calculated and difference profiles (continuous lines), and reflection positions (|).Goodness of fit values of Fitted R_{wp} = 0.0113, Fitted R_p = 0.0085, Reduced χ^2 = 1.462 reflect the excellent agreement between the model and data.

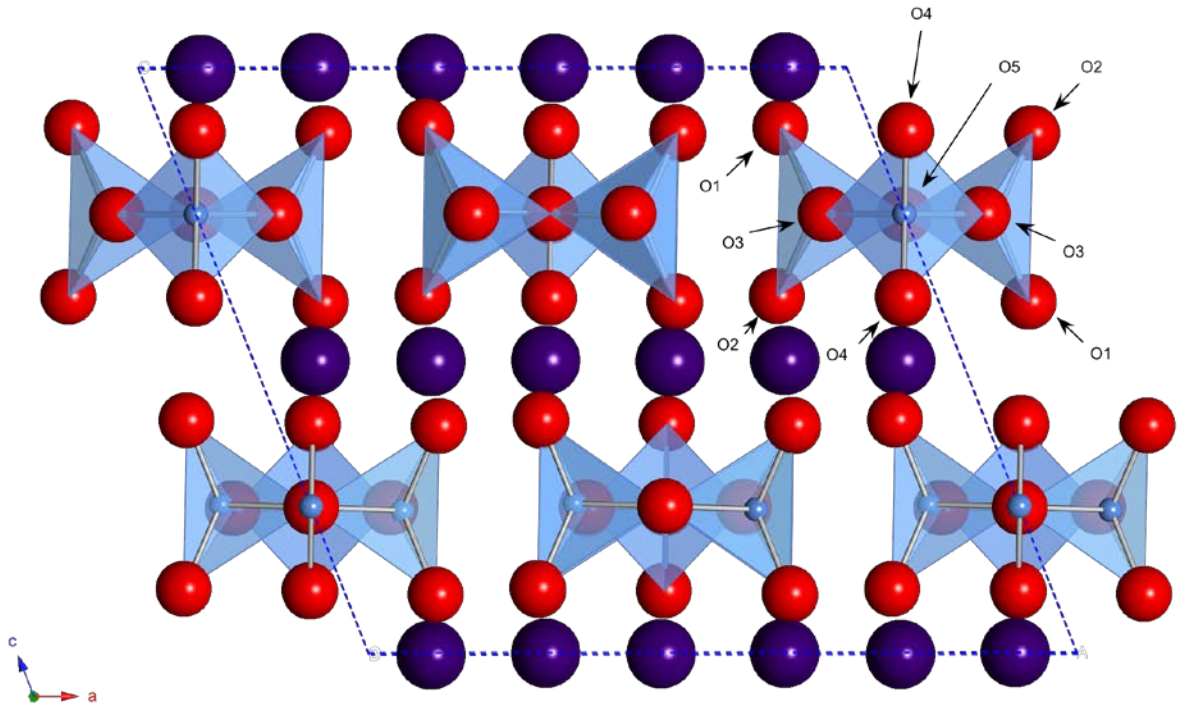

Figure 2. Crystal structure of $SrSiO_3$, the blue tetrahedra highlight the corner sharing Si-O layers and the purple spheres layers of Sr. The crystallographically independent oxygen sites have been labelled.

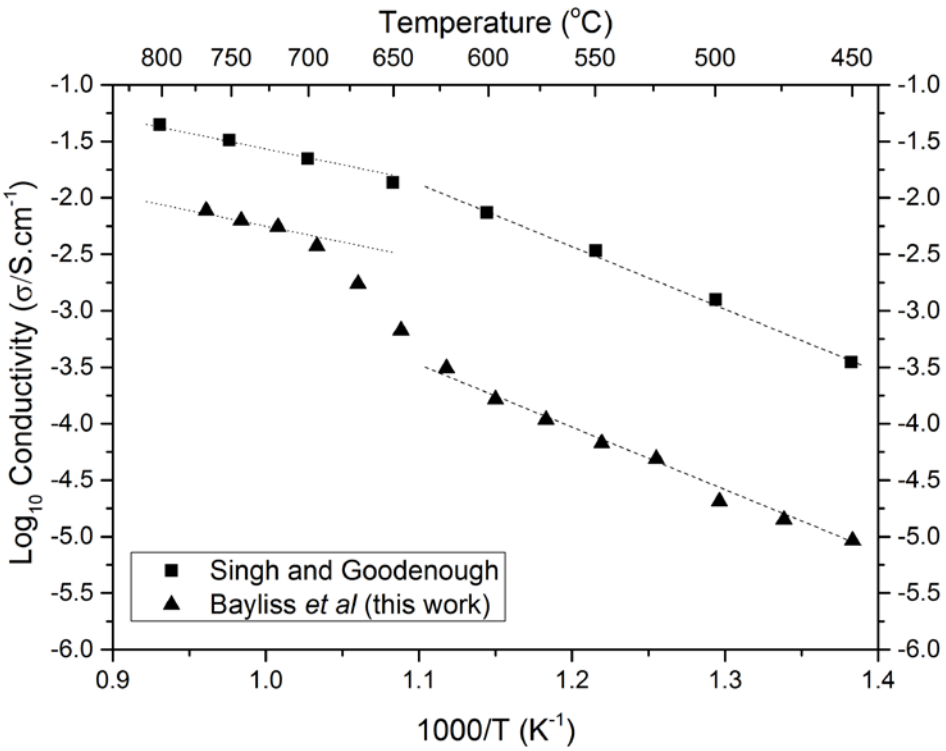

Figure 3. Arrhenius plot of total conductivity from literature values[1] and those from this work as a function of reciprocal temperature. The figure highlights the change in Ea in both data sets and the difference in total conductivity between the work reported in the literature and recorded during this work.

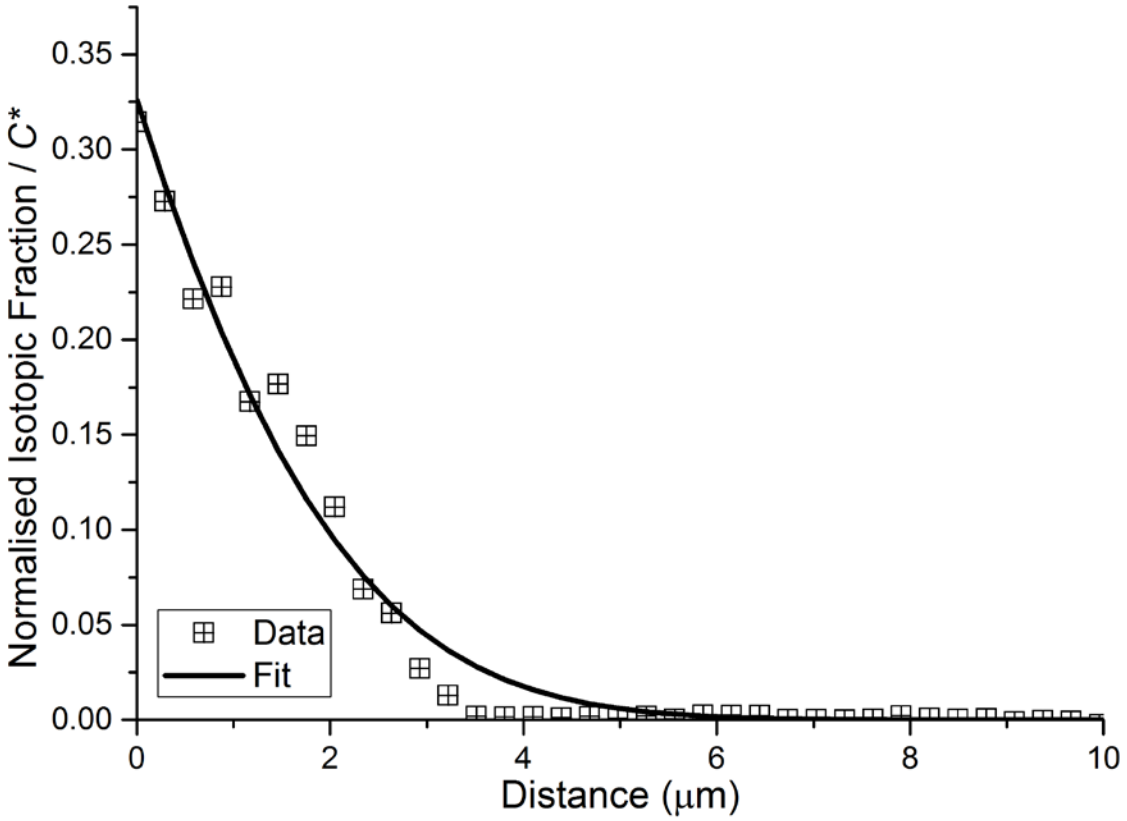

Figure 4. ^{18}O oxygen tracer diffusion profile of a pellet of nominal composition, $Sr_{0.8}K_{0.2}Si_{0.5}Ge_{0.5}O_{2.9}$ at 737 °C for 72 minutes. The surface of the polished pellet was catalysed by porous Pt to enhance oxygen exchange, which is reflected in the high surface concentration.

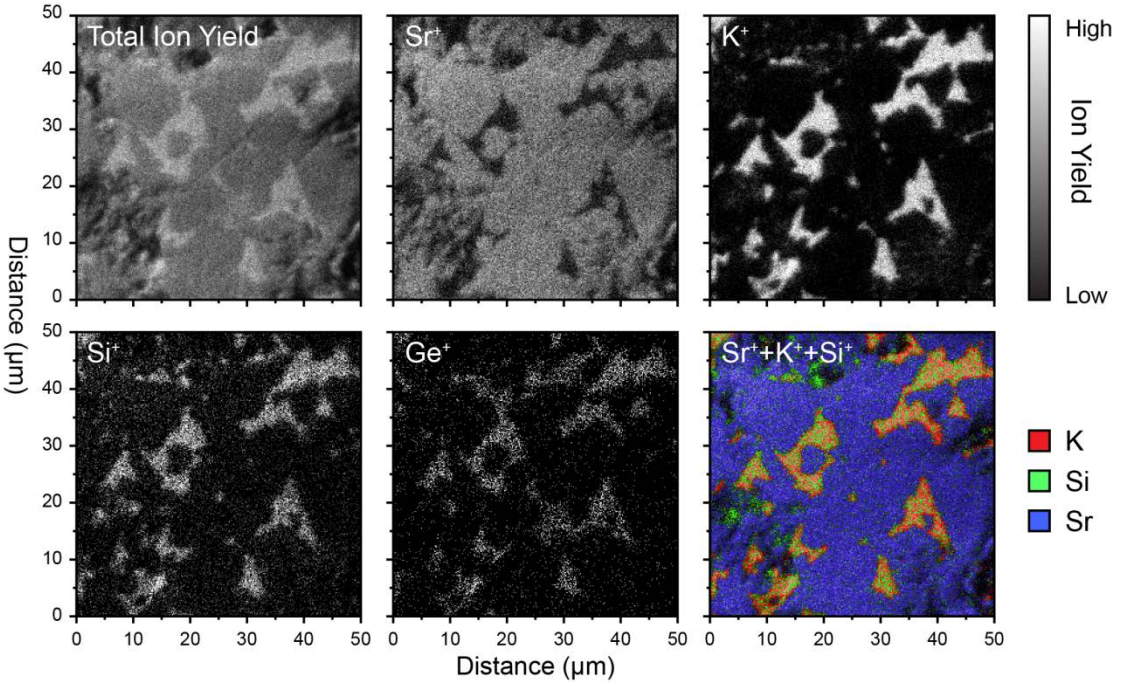

Figure 5. ToF-SIMS **c**hemical ion mapping over an area of 50 × 50 μm^2, clearly showing an inhomogeneous elemental distribution.

Element	*x*	*y*	*z*	Multi	Fraction
Sr 1	0.0867(2)	0.2410(2)	0.4992(3)	8	0.97(1)
Sr 2	0.25	0.25	0	4	0.97(1)
Si 1	0.1264(2)	0.4551(3)	0.2457(2)	8	0.53(1)
Ge 1	0.1264(2)	0.4551(3)	0.2457(2)	8	0.47(1)
Si 2	0	0.8384(5)	0.25	4	0.59(2)
Ge 2	0	0.8384(5)	0.25	4	0.41(2)
O 1	0.1265(2)	0.4076(4)	0.1005(2)	8	0.97(1)
O 2	0.2254(2)	0.4047(5)	0.3893(2)	8	0.98(1)
O 3	0.1094(2)	0.6926(4)	0.2484(2)	8	0.97(1)
O 4	0.0483(2)	0.9372(5)	0.3924(2)	8	1
O 5	0	0.3605(5)	0.25	4	0.96(1)

Element	U11*100	U22*100	U33*100	U12*100	U13*100	U23*100
Sr 1	0.1(1)	0.5(1)	0.2(1)	0.6(1)	-0.2(1)	0.8(1)
Sr 2	0.5(2)	0.8(2)	0.9(3)	-0.3(2)	0.6(2)	-0.1(2)
Si/Ge 1	0.6(1)	0.1(1)	0.5(1)	0.1(1)	-0.3(1)	-0.3(1)
Si/Ge 2	2.1(3)	1.6(3)	0.6(3)	0	0.7(2)	0
O 1	1.1(2)	0.3(1)	0.5(1)	0.6(1)	0.4(1)	0.4(1)
O 2	0.8(2)	0.4(2)	1.3(1)	-0.2(1)	0.5(1)	-0.2(2)
O 3	0.9(2)	0.2(2)	1.1(2)	0.1(1)	0.4(1)	-0.2(1)
O 4	2.1(2)	0.5(2)	1.4(1)	-0.3(1)	1.0(1)	-0.3(1)
O 5	0.6(3)	1.2(3)	1.4(3)	0	0.6(2)	0

Table 1. Final structural parameters for K absent ~$SrSi_{0.5}Ge_{0.5}O_3$ obtained from ambient temperature time-of-flight NPD data showing final atomic coordinates, site multiplicity and fractional occupancy of sites. O4 refined to full occupancy so was fixed at 1. Final anisotropic atomic displacement parameters are also presented, those for the mixed Si/Ge cation sites were constrained as equivalent. Space group C2/c.